The Journal of Pathology: Clinical Research
J Pathol Clin Res October 2018; **4:** 227–240
Published online in Wiley Online Library
(wileyonlinelibrary.com). DOI: 10.1002/cjp2.105

ORIGINAL ARTICLE

Replacement and desmoplastic histopathological growth patterns: A pilot study of prediction of outcome in patients with uveal melanoma liver metastases

Raymond Barnhill[1,2*], Peter Vermeulen[3,4], Sofie Daelemans[3,4], Pieter-Jan van Dam[3,4], Sergio Roman-Roman[5], Vincent Servois[6], Ilse Hurbain[7,8,9], Sophie Gardrat[1], Graça Raposa[7,8,9], André Nicolas[1], Rémi Dendale[10], Gaëlle Pierron[11], Laurence Desjardins[12], Nathalie Cassoux[2,12], Sophie Piperno-Neumann[13†], Pascale Mariani[14†] and Claire Lugassy[5]

[1]*Department of Pathology, Institut Curie, Paris, France*
[2]*University of Paris Réné Descartes Faculty of Medicine, Paris, France*
[3]*HistoGeneX, Antwerpen, Belgium*
[4]*Faculty of Medicine and Health Sciences, University of Antwerp – MIPRO Center for Oncological Research (CORE) - TCRU, GZA Sint-Augustinus, Antwerpen, Belgium*
[5]*Department of Translational Research, Institut Curie, Paris, France*
[6]*Department of Radiology, Institut Curie, Paris, France*
[7]*Institut Curie, PSL Research University, CNRS, Paris, France*
[8]*Sorbonne Universités, UPMC Univ Paris 06, CNRS, Paris, France*
[9]*Cell and Tissue Imaging Core Facility PICT-IBiSA, Institut Curie, Paris, France*
[10]*Department of Radiotherapy, Institut Curie Orsay, Paris, France*
[11]*Department of Somatic Genetics, Institut Curie, Paris, France*
[12]*Department of Ophthalmology, Institut Curie, Paris, France*
[13]*Department of Medical Oncology, Institut Curie, Paris, France*
[14]*Department of Surgery, Institut Curie, Paris, France*

**Correspondence to: Raymond L. Barnhill, Department of Pathology, Institut Curie, 26 rue d'Ulm, 75248 Paris cedex 05, France.*
E-mail: raymond.barnhill@curie.fr

[†]*Equivalent contributors.*

Abstract

Up to 50% of uveal melanomas (UM) metastasise to the liver within 10 years of diagnosis, and these almost always prove rapidly fatal. As histopathological growth patterns (HGPs) of liver metastases of the replacement and desmoplastic type, particularly from colon and breast carcinoma, may import valuable biological and prognostic information, we have studied HGP in a series of 41 UM liver metastases originating from 41 patients from the period 2006–2017. Twenty patients underwent enucleation while 21 had radiation therapy. Analysis of UM by array comparative genomic hybridisation revealed: 25 (64%) patients with high risk (monosomy3/8q gain); 13 (33%) intermediate risk (M3/8normal or disomy3/8q gain); and 1 low risk (disomy3/8normal). The principal HGP was replacement in 30 (73%) cases and desmoplastic in 11 (27%) cases. Cases with replacement demonstrated striking vascular co-option/angiotropism. With the development of liver metastasis, only the replacement pattern, largest primary tumour diameter, and *R*2 (incomplete resection) status predicted diminished overall survival (OS; $p < 0.041$, $p < 0.017$, $p < 0.047$, respectively). On multivariate analysis, only HGP (hazard ratio; HR = 6.51, $p = 0.008$) and resection status remained significant. The genomic high-risk variable had no prognostic value at this stage of liver metastasis. Chi-square test showed no association of HGP with monosomy 3 or 8q gain. Eighteen of 41 (44%) patients are alive with disease and 23 (56%) patients died with follow-up ranging from 12 to 318 months (mean: 70 months, median: 47 months). In conclusion, we report for the first time the frequency of the replacement and desmoplastic HGPs in liver UM metastases resected from living patients, and their potential important prognostic value for UM patients, as in other solid cancers. These results may potentially be utilised to develop radiological correlates and therapeutic targets for following and treating patients with UM metastases.

Keywords: uveal melanoma; metastasis; liver; histopathological growth patterns; replacement; desmoplastic; vascular co-option; angiotropism

Received 15 February 2018; Revised 7 June 2018; Accepted 8 June 2018

Conflict of interest statement: Peter Vermeulen, Sofie Daelemans and Pieter-Jan van Dam are part- or full-time employees of HistogeneX. The other authors declare no conflict of interest.

Abbreviations

array CGH	array comparative genomic hybridisation
D3	Disomy 3, no loss of chromosome 3
EVMM	Extravascular migratory metastasis
HGP	histopathological growth pattern
LTD	largest tumour diameter (primary uveal melanoma)
MD	Missing Data
MRI	Magnetic resonance imaging
M3	monosomy 3, loss of chromosome 3
UM	uveal melanoma
8g	gain in chromosome 8q
8nl	8 chromosome normal, absence of 8q gain
8q	long arm of chromosome 8

Introduction

Up to 50% of uveal melanomas (UM) metastasise to the liver within 10 years of diagnosis, and these almost always prove rapidly fatal [1]. Despite considerable progress in defining the molecular phenotype of UM [2], the mechanisms of UM metastasis remain poorly understood [1]. Although it has long been assumed that haematogenous spread accounts for virtually all UM metastasis, liver metastases may appear months to many years after diagnosis of the primary tumour [3,4]. This temporal variation and latency in the appearance of metastases could be explained by (1) the formation of dormant metastases after intravascular spread [5,6] and/or (2) extravascular migratory metastasis (EVMM), or step-by-step migration from the primary tumour to the site of metastasis [7–9]; this has also been reported in other tumours [10–13]. Tumour cell dormancy in UM may be secondary to a number of mechanisms, such as escape from immune surveillance in the space of Disse [4,5], angiogenesis [14], or tumour cell kinetics [5].

Dormant UM metastases have been suggested by microscopic foci of melanoma cells in autopsy samples from patients with UM liver metastases [5]. In another autopsy study of 10 patients [15], UM liver metastases were categorised into three stages: stage I, deposits ≤50 μm in diameter, and stage II, deposits 51–500 μm, both within sinusoidal spaces; and stage III, deposits ≥500 μm. Stage III metastases showed two distinct growth patterns which were termed 'lobular' and 'portal'. In a subsequent study of 15 autopsy cases, the latter observations were extended and the term *infiltrative* growth pattern proposed to replace 'lobular' and *nodular* to replace 'portal' growth patterns in liver metastases from UM [4]. The 'infiltrative' pattern was characterised by nondestructive growth of melanoma cells into the surrounding hepatic parenchyma with eventual expansile growth. In the nodular pattern, melanoma cells were initially aligned along portal venules and subsequently formed cohesive nodules obliterating the architecture of the liver. These observations have recently been supplemented by core liver biopsies and correlation with radiographic images [16].

The investigation of hepatic UM metastases is challenging as it is difficult to obtain adequate material for research. In particular, satisfactory autopsy material and sufficiently large liver samples of metastatic UM resected from living patients are rare.

Conversely, the liver is a frequent site of metastasis for tumours originating from the gastrointestinal tract, pancreas, breast, and lung but also not uncommonly from renal cell carcinoma, various sarcomas, and cutaneous melanoma [17–21]. Liver metastases from colon and breast cancers have been extensively studied and show distinctive 'histopathological growth patterns' (HGPs) [19–21]. In brief, these HGPs are: 'replacement', 'desmoplastic', 'pushing', and two rare variants – the 'sinusoidal' and 'portal' HGPs. The HGPs are represented by a distinctive interface between cancer cells and the adjacent normal liver parenchyma that can be recognised by conventional microscopy (Figure 1). In brief, the replacement HGP is defined by tumour cells from the metastasis infiltrating and forming plates in continuity with the surrounding hepatic parenchymal plates and perpendicular to the tumour–liver interface (Figure 1A); the desmoplastic HGP by a distinct separation of the metastasis by a peripheral annulus (rim) of desmoplastic fibrous tissue (Figure 1B); the pushing pattern by compression and pushing away of hepatic plates by the metastasis without tumour cells invading the liver plates (Figure 1C); the sinusoidal pattern by the presence of tumour cells in sinusoidal blood vessels or peri-sinusoidal spaces in between the liver plates; and the portal pattern by the metastasis being restricted to the portal tracts [21]. The distinctive topography of cancer cells in each HGP predicts HGP-specific interactions with parenchymal cells (hepatocytes and cholangiocytes) and nonparenchymal cells (sinusoidal endothelial cells, stellate cells, and immune cells) of the liver. Importantly, the HGPs of liver metastases from these tumours have prognostic significance [19–22].

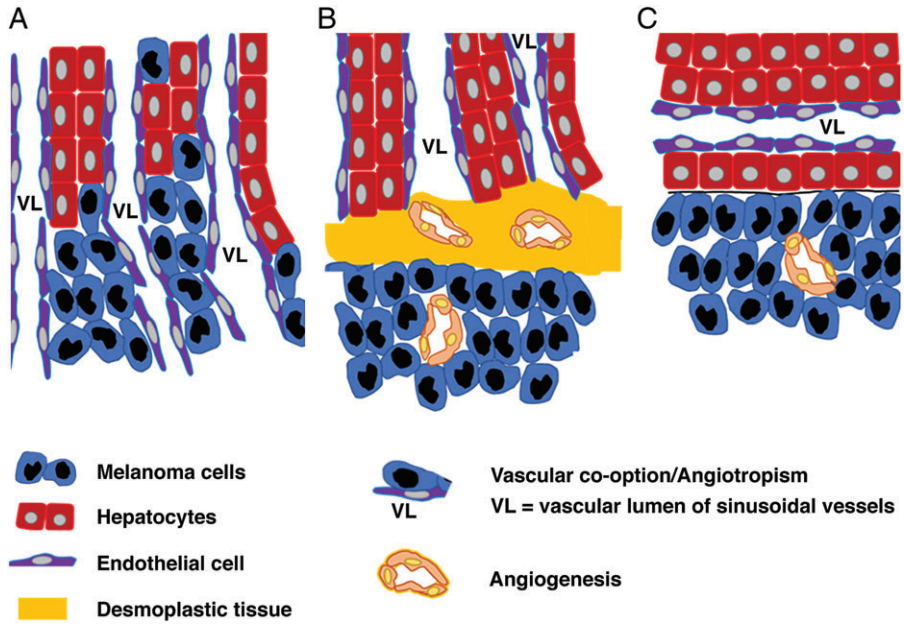

Figure 1. Histopathological growth patterns. (A) Replacement histopathological growth pattern: melanoma cells (blue) invade the liver cell plates, replace the hepatocytes (red), and co-opt the sinusoidal blood vessels (purple endothelial cells). There is no angiogenesis. VL, vascular lumen of sinusoidal vessels. (B) Desmoplastic histopathological growth pattern: melanoma cells (blue) are separated from the liver (red hepatocytes) by a rim of desmoplastic tissue (yellow) which contains newly formed blood vessels (angiogenesis, orange endothelial cells). Melanoma cells do not invade the liver cell plates. (C) Pushing histopathological growth pattern: melanoma cells (blue) push away the liver cell plates (red hepatocytes) and do not invade the liver cell plates. New blood vessels (angiogenesis, orange endothelial cells) are formed in the metastasis.

One of the most important observations made in these studies is that liver metastases with a replacement HGP do not rely on sprouting angiogenesis for a vascular supply but instead 'co-opt' the sinusoidal vasculature of the liver [17–22]. This is inferred from the specific morphology of replacement type liver metastases and is consistent with the low endothelial cell proliferation fraction reported in these metastases. Conversely, the desmoplastic HGP is associated with an 'angiogenic' phenotype [17–22].

In cutaneous melanoma, we have described the association of tumour cells with the abluminal surfaces of vascular channels, which is termed angiotropism [23,24]. Importantly, we have shown in a recent study that the terms 'co-option' and 'angiotropism' appear to connote the same phenomenon [25]. Angiotropic tumour cells can spread along the abluminal surfaces of vessels without entering the vascular channels (intravasation), therefore making use of the blood vascular network as a track [7–9,25]. As mentioned earlier, this tumour cell migration has been termed EVMM and is believed to represent a mechanism of tumour spread independent of intravasation and haematogenous dissemination [7].

Extraocular tumour extension of UM has been extensively described [26–32]. In primary UM, we have recently observed that extraocular tumour extension along vessels, or angiotropism/co-option, is strongly associated with the development of metastases and death [33]. In UM, angiotropism and extravascular spread of melanoma refers specifically to migration of tumour cells along the abluminal basement membranes of vascular endothelial cells within the emissary canals of the sclera [for detailed discussion see Barnhill *et al* 33]. Because of the biological and prognostic importance of angiotropism in melanoma in general [7–9,33–35], and also because of the adverse prognostic value of the replacement HGP (co-option/ angiotropism) in other solid tumours [19–22], we have undertaken new investigations of liver metastases from UM.

Herein we have examined, by conventional microscopy, surgically sampled liver metastases from 41 patients with UM, in order to determine if specific HGPs are present in UM liver metastases. Immunohistochemistry and electron microscopy (EM) were performed on selected cases.

Materials and methods

This study was approved by the institutional ethics committee of Institut Curie. Written informed consent

for the use of tissue specimens and data for research was signed by each patient. The study complied with the principles of the Declaration of Helsinki.

Patient information

Forty-one hepatic metastases from 41 patients with UM were retrieved from the anatomic pathology archives of the Institut Curie from the period 2006–2017. Clinical, histopathological, molecular genetic, and long-term follow-up information for these patients has been collected prospectively as previously described [36]. The following patient characteristics were analysed and most variables are displayed in Table 1: age (years); gender; laterality; largest tumour diameter (LTD) of the primary melanoma (mm); melanoma cell type (modified Callender classification [37]): epithelioid, spindle, or mixed [33,36]; local extension of the primary tumour (ciliary body, optic nerve, or extrascleral extension); genetic analysis (see below); local therapy of the primary melanoma [proton beam therapy, radioactive (iodine) disc brachytherapy, and enucleation]; disease-free interval (time to metastasis); R (resection) status of metastasis: *R*0 – resection complete, *R*1 – microscopically incomplete, and *R*2 – macroscopically incomplete; initial therapy of liver metastases (surgery alone, surgery plus systemic therapy, and any systemic therapy); and overall survival (OS).

Histopathology

Formalin-fixed, paraffin-embedded (FFPE) 5-µm sections were prepared for each liver metastasis for microscopic examination. Whole glass slides were digitised with a Phillips pathology slide scanner (Phillips Healthcare, Amsterdam, The Netherlands). Criteria for the selection of metastases were as follows: if more than one metastasis was present, criteria for selection included metastases having a 360° circumference surrounded by viable intact liver parenchyma, or those with the highest percentage of the peripheral circumference (of the metastasis) surrounded by liver parenchyma, and absence of significant necrosis, scarring, or disruption of either the metastasis or the liver. Histopathological characteristics recorded based on the examination of representative haematoxylin and eosin-stained sections or digital images for each case included: the HGP of the liver metastases; diameter of each metastasis (mm); and angiotropism of melanoma cells. The HGP was scored according to consensus guidelines as described by van Dam *et al* [21]. The liver metastasis HGP assessment consisted of the percentage of the circumference involved (at least 5%) by desmoplastic, replacement, or pushing HGP. The dominant HGP (≥50% of the circumference) was used for further analyses. Angiotropism was defined as previously described [7,33].

Table 1. Patient characteristics

Patient characteristics	*n* = 41 (%)
Gender (female)	21 (51%)
Age at diagnosis (years)	
Mean (SD)	54 (11.7)
Median (range)	55 (30–76)
Laterality of primary melanoma (*n* = 41)	
Left eye	27 (66%)
Right eye	14 (34%)
Primary tumour characteristics	***n* = 41 (%)**
Largest tumour diameter (LTD) (mm) (MD = 3)	
Mean (SD)	16.6 (2.9)
Median (range)	17 (10–23)
Melanoma cell type (*n* = 20) (no MD)	
Epithelioid	6 (30%)
Spindle	5 (25%)
Mixed	9 (45%)
Local extension (no MD)	
Ciliary body	10 (24%)
Optic nerve	1
Extrascleral	0
***Array CGH (*n* = 39) (MD = 2)**	
D3/8nl	1 (2.6%)
M3/8nl	5 (13%)
D3/8g	8 (20%)
M3/8g	25 (64%)
Local treatment (no MD)	
Proton beam	19 (46%)
Iodide disc brachytherapy	2 (5%)
Enucleation	20 (49%)
Fine-needle aspiration	9 (22%)
Disease-free interval *(time to metastasis) (months)*	
Mean (SD)	44 (52)
Median (range)	25 (7–290)
First treatment of mets/*R* status (*R* status MD = 1)	
R0 surgery	20 (50%)
R1 surgery	4 (10%)
R2 systemic	16 (40%)
Overall survival from diagnosis of mets (months) (MD = 2)	
Mean (SD)	26 (19.8)
Median (range)	23 (5–101)
First treatment: surgery alone (months)	*n* = 6
Mean (SD)	30 (18.1)
Median (range)	25 (14–66)
Surgery + systemic treatment (months)	*n* = 21
Mean (SD)	29 (23.9)
Median (range)	23 (6–101)
Any systemic treatment (months)	*n* = 14
Mean (SD)	20 (11.3)
Median (range)	18 (5–48)

*Array CGH: 11/41 (27%) did not undergo fine needle aspiration biopsy of the primary tumour or had no contributive primary tumour sample for analysis. However, the genomic analysis of liver metastases was performed in nine of these remaining patients. No tissue was available for two patients. MD = missing data.

Angiotropism was defined as melanoma cells arrayed along the abluminal vascular surfaces of sinusoidal vessels (in the space of Disse) and/or along portal venules in the portal tracts. In particular, this included (1) clearly recognisable (unequivocal) melanoma cells disposed circumferentially, radially, or longitudinally along the abluminal (external) surfaces of the endothelium of microvascular channels either in single-layered or multi-layered arrangements; (2) the latter occurring in at least one or more foci; and (3) there was no evidence of intravascular melanoma cells.

The images were reviewed independently by two experienced senior pathologists (P.V. and R.B.) without specific knowledge of the case or clinical outcome.

Genetic analysis

Among the 41 patients, 39 had sufficient tumour from frozen tissue samples for array comparative genomic hybridisation (aCGH), as previously described [36]. Metastatic samples were utilised if no primary melanoma tissue was available. Two patients had no primary or metastatic tumour available. In brief, 43 tumour samples from 20 enucleations, 9 fine-needle aspirations, and 14 resected liver metastases, including 6 cases with material from both primary tumours and liver metastasis, were studied. Among the 14 frozen samples from the liver, two were excluded because of inadequate aCGH results. Only the status of chromosomes 3 and 8 (8q) was assessed.

The risk for the development of metastasis in patients with four genomic profiles was analysed. These Cassoux risk groups [36] were defined by the presence or absence of chromosome 3 loss (monosomy 3) *and* the presence or absence of chromosome 8 gain (including gain of the entire 8 chromosome, gain of the entire 8q, and distal gain of 8q), as follows: Cassoux risk group 1, Low risk for metastasis: normal status of chromosomes 3 (disomy 3) and 8 (8nl): D3/8nl; Group 2, Intermediate risk: monosomy 3 and normal status of 8: M3/8nl; Group 3, Intermediate risk: disomy 3 and gain of 8q (8g): D3/8g; and Group 4, High risk: M3/8g (Tables 1 and 3) [36].

Immunohistochemistry

FFPE sections from five metastases showing a replacement HGP were examined by immunohistochemistry with HMB45 [Dako (Dako Agilent, Santa Clara, CA, USA), clone M0823, dilution 1/100]. Double immunostaining with both HMB45 and CD31 (Dako, clone JC70A, dilution 1/100) was performed on three of these five cases. A Vector Red chromogen (Vector Laboratories, Burlingame, CA, USA) was utilised for HMB45 and diaminobenzidine (DAB) for CD31. Peroxidase activity was developed using 3-amino-9-ethylcarbazole and H_2O_2, and the slides were counterstained with hematoxylin.

Electron microscopy

For EM, three samples from liver metastases originating from primary UM were fixed overnight in 1.5% glutaraldehyde at 4°C. Samples were then embedded in epoxy epon 812 resin (Shell) (EPON) and thin sections of 60–70 nm were post stained with 4% aqueous uranyl acetate for 10 min and lead citrate for 1 min. Electron micrographs were acquired on a Tecnai Spirit electron microscope (Thermo Fisher Scientific, Eindhoven, The Netherlands) equipped with a 4k CCD camera (Quemesa, EMSIS GmbH, Münster, Germany).

Correlation of angiotropism in primary UM with HGP in liver metastasis

Eight UM patients with liver metastases in the present study were derived from a previous study of 89 primary UM evaluated for angiotropism [33]. The presence or absence of angiotropism in the primary UM was correlated with replacement or desmoplastic growth pattern.

Statistical analyses

Data were analysed using R statistical software (https://cran.r-project.org). The relationships between HGP and other categorical variables were evaluated by the Chi-square test. The survival analyses included OS, 5-year survival, and disease-free (metastasis-free) survival (DFS). Patients were censored when alive at last follow-up or when lost to follow-up. OS was defined as the difference between time of metastasis (OS metastasis) and time of death or last follow-up or the difference between time of diagnosis of the primary UM (OS primary) and time of death or last follow-up. Differences in survival were calculated using log-rank test. Univariate and multivariate hazard ratios (HR) were calculated using Cox proportional hazards model. All statistical tests were considered significant with P value <0.05. As we did not know if there was any effect among the Cassoux risk scores, the HGP, and the other clinical variables, we opted to keep all the variables in the multivariate analysis in order to adjust for confounding and suppression of variables in our data set [38]. Removing the variables that were not significant in univariate analysis could lead to the exclusion of possible significant variables due to suppression.

Results

Patient and primary melanoma characteristics

The patient clinical information and primary tumour characteristics are summarised in Table 1.

Primary melanoma tumour diameter was mean = 16.6 mm, median = 17 mm (range: 10–23 mm). Genetic analysis revealed: D3/8nl: 1 patient (2.6%), D3/8g: 8 (20.5%), M3/8nl: 5 (13%), M3/8g: 25 (64%). Four patients with satisfactory results from aCGH analysis of both the primary UM and the corresponding liver metastasis showed complete concordance of the genomic profiles of their primary tumour and their paired liver metastasis.

Eighteen of 41 (44%) patients are alive with disease and 23 (56%) patients died with a follow-up ranging from 12 to 318 months (mean: 70 months, median: 47 months). Two patients have been lost to follow-up. Four patients with previously treated metastatic disease currently have no evidence of disease. The mean and median DFS intervals were 44 and 25 months, respectively, with a range of 7–290 months. OS after the development of liver metastases averaged 26 months with a median of 23 months and range of 5–101 months. OS after the following therapies for metastatic disease were: surgery alone – mean 30 months, median 25 (range 14–66); surgery plus systemic therapy – mean 29 months, median 23 (range 6–101); systemic therapy alone – mean 20 months, median 18 (range 5–48) ($p > 0.05$).

Categorisation of metastases by HGP

Analysis of HGP and diameter of metastases are summarised in Table 2. Initial independent blinded review of the HGP in the 41 metastases by the two pathologists revealed good to excellent general agreement for 31 cases, whereas 10 cases (24% of the 41 cases) resulted in some initial discordance. The pathologists reached concordance by the following measures: (1) in a few cases, a suboptimal glass slide or image was replaced by another slide or image which resulted in concordance by both pathologists, and (2) the few remaining problematic cases were reviewed and discussed by webinar and final consensus reached during these discussions. Twenty-five metastases had a pure (100%) replacement pattern, 4 metastases a pure (100%) desmoplastic pattern, 5 metastases a predominant (>50%) replacement and <50% desmoplastic pattern, and 7 metastases a predominant (>50%) desmoplastic and <50% replacement pattern. In 26 of 41 cases, at least 10 level sections were obtained, and the predominant HGP did not change in any case. In the remainder of the cases, at least one section (1–5 sections) were examined for each case and there was no change in HGP. For statistical analysis, the metastases were categorised as predominant HGP (Table 2). As a group, the metastases ranged in size from 1 to 17 mm in diameter with mean of 6.6 mm and median of 5 mm, and there was no significant difference in size between the replacement and desmoplastic metastases ($p = 0.23$ using Mann–Whitney U-test).

Table 2. Characteristics of liver metastases

Histopathological growth patterns	$n = 41$ (%)
Pure versus mixed pattern	
Replacement (pure, 100%)	25 (61%)
Desmoplastic (pure, 100%)	4 (10%)
Mixed (replacement, desmoplastic, or pushing)	12 (29%)
Predominant pattern (>50%)	
Replacement (>50%)	30 (73%)
Desmoplastic (>50%)	11 (27%)
Metastasis diameter	**$n = 41$**
Metastasis diameter (mm) ($n = 41$)	
Mean (SD)	6.6 (4.7)
Median (range)	5 (1–17)
Replacement diameter (mm) ($n = 30$)	
Mean (SD)	6.4* (4.8)
Median (range)	4.5 (1–17)
Desmoplastic diameter (mm) ($n = 11$)	
Mean (SD)	7.4* (4.7)
Median (range)	6 (3–15)

*No difference in size ($p = 0.23$ using Mann–Whitney U-test).

Approximately three quarters (73%) of the metastases showed a predominant replacement HGP. These metastases were characterised by nondestructive infiltration of the surrounding liver hepatic plates, progressive replacement of hepatocytes by melanoma cells (Figure 2) and preservation of the liver architecture (Figures 2B,C). Individual melanoma cells, usually identified by cytoplasmic melanin, appeared to be aligned along the external (abluminal) surfaces of the sinusoidal vascular channels. A striking feature associated with many of these metastases was the radial extension of individual melanoma cells considerable distances (up to 1 mm) away from the central metastatic focus into the surrounding liver parenchyma (Figure 2B–D). The melanoma cells continued to show an apparent localisation along the abluminal surface of sinusoidal vessels, corresponding to the Space of Disse. Within many of these metastases, one could observe a complete replacement of hepatocytes by melanoma cells in the hepatic plates. In no instance was there clear evidence of melanoma cells within the lumina of the sinusoidal vessels. Within the portal triads of some of these metastases, melanoma cells were disposed along the abluminal surfaces of portal venous vessels (angiotropism). In such metastases, variable perivascular lymphocytic infiltrates were often seen.

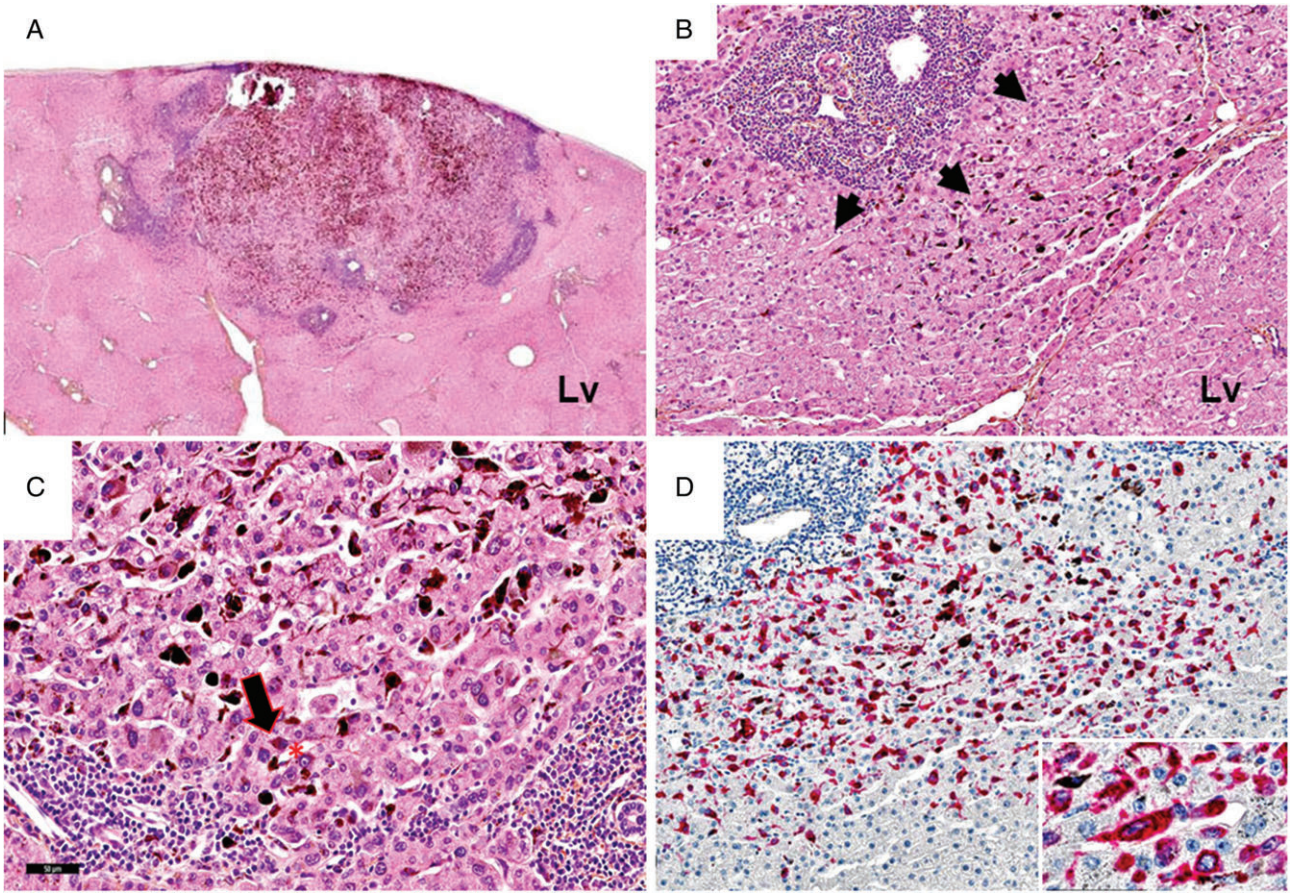

Figure 2. Replacement histopathological growth pattern. (A) Scanning magnification shows a discrete metastasis abutting the liver capsule. Lv, surrounding uninvolved liver parenchyma. (B) The interface (broad zone extending from upper right quadrant to lower left quadrant) between the metastasis (upper left quadrant) and surrounding liver parenchyma (Lv) (lower right quadrant) is poorly defined. Melanoma cells (detected by the presence of cytoplasmic melanin and cytological atypia) are dispersed throughout this peripheral interface as single cells (arrowheads) and small clusters beyond the main portion of the metastasis. These cells replace hepatocytes in the hepatic plates without altering their architecture. (C) Melanoma cells (arrow) extending into the surrounding hepatic plates some distance from the metastasis along the sinusoidal vessels. Red asterix indicates vascular lumen. Black arrow identifies melanoma cells. (D) HMB45 immunostain with red chromogen highlights melanoma cells extending into the surrounding liver parenchyma. Inset; Melanoma cells expressing HMB45 are disposed along the abluminal endothelial surface of a sinusoidal vessel in the hepatic parenchyma. The endothelial cell lining is highlighted by CD31 (DAB brown chromogen).

Approximately a quarter of the metastases showed a predominant desmoplastic HGP. These tumours were well-circumscribed with complete separation of the metastasis from the surrounding liver parenchyma by an annulus of dense desmoplastic collagen (Figure 3). Within the metastatic nodule, there was a complete obliteration of the liver architecture. In general, these metastases showed prominent peri-tumoural infiltrates of lymphocytes localised to the desmoplastic-liver parenchymal interface (Figure 3C). Usually, tumour-infiltrating lymphocytes were sparse or absent.

Three metastases were classified as mixed with the presence of all three HGPs: desmoplastic, replacement, and pushing [21]. However, the pushing HGP in each instance involved only a small fraction of the circumference of the metastasis: 20, 5, and 5%, and the prevailing pattern was desmoplastic or replacement.

Immunohistochemistry

Immunohistochemical evaluation of three replacement metastases showed striking localisation of melanoma cells within hepatic plates along the external surfaces of the sinusoidal vascular channels (Figure 2D). This vascular-co-option/angiotropism was best visualised at the metastasis-liver

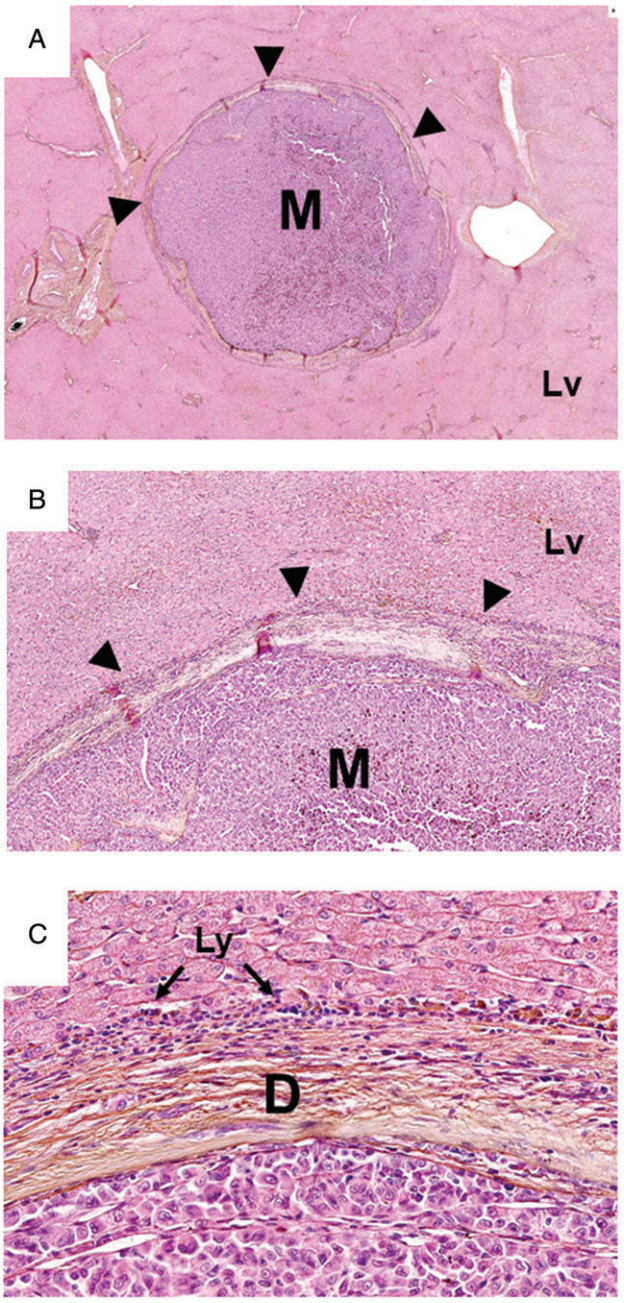

Figure 3. Desmoplastic histopathological growth pattern. (A) Small round metastasis (M) with abrupt desmoplastic interface (arrowheads) separates the tumour from the surrounding liver parenchyma. The liver architecture is completely obliterated by the tumour mass. Lv, surrounding uninvolved liver parenchyma. (B) An annulus of dense desmoplastic collagen constitutes this interface (arrowheads). Liver parenchyma (Lv) is observed in the upper half of this field and the metastasis (M) in the lowermost portion of the field. (C) High magnification of B. Note the rim of peri-tumoural lymphocytes (Ly), which are at the interface of the desmoplastic annulus (D) and the surrounding liver parenchyma.

parenchymal interface and in the immediately surrounding peri-tumoural liver parenchyma. There was no clear-cut evidence of melanoma deposits within the sinusoidal vascular lumina. As mentioned earlier, melanoma labelling with HMB45 showed a striking angiotropism to the abluminal surfaces of portal venules in the portal triads of some metastases. Double immunohistochemistry with HMB45 and CD31 showed variable but generally weak labelling of sinusoidal endothelial cells and localisation of melanoma cells to the external (abluminal) surfaces of both sinusoidal and portal vascular channels (Figure 2D inset) without objective evidence of intraluminal melanoma cells.

Electron microscopy

Two replacement pattern metastases were studied by EM. Examination of these specimens in the peritumoural regions revealed melanoma cells external to the endothelial lining of sinusoidal vessels (Figure 4). Melanoma cells were definitively identified by the presence of melanosomes.

Correlation of angiotropism in primary UM with HGP in liver metastasis

Among four primary UM with angiotropism [33], three primary UM demonstrated a replacement pattern in the liver metastasis and one a desmoplastic pattern. Two primary UM with absence of angiotropism manifested a desmoplastic HGP. For two metastases with

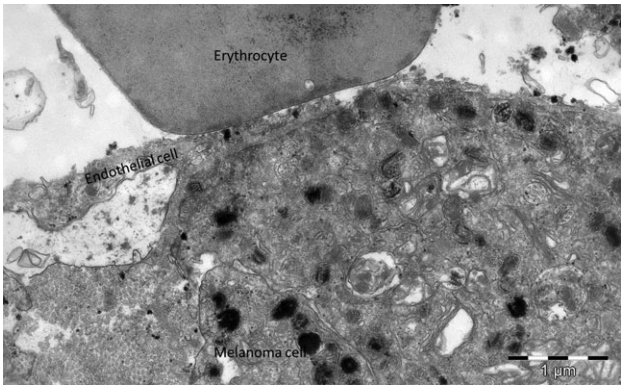

Figure 4. Electron microscopy of replacement HGP. This field shows the lumen of a sinusoidal vascular channel (upper third of field) which contains an erythrocyte and exhibits an attenuated endothelial cell lining. A melanoma cell (in the lower two-thirds of the field) is identified by cytoplasmic melanosomes (dense bodies). The melanoma cell is disposed along the abluminal surface of the sinusoidal vessel.

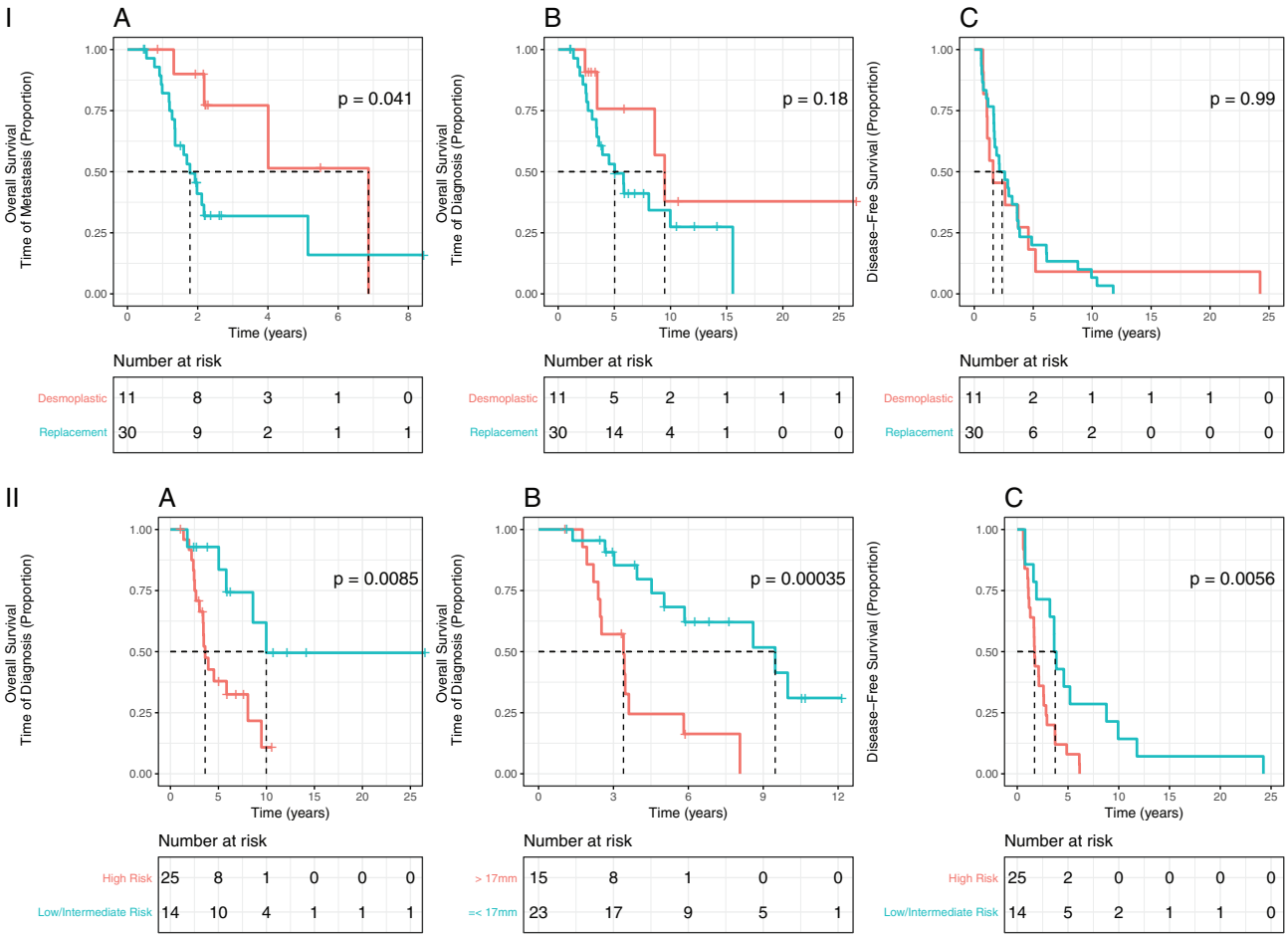

Figure 5. (I) The effects of replacement and desmoplastic HGPs of UM liver metastases on overall survival analysed by the Log Rank test with Kaplan–Meier plots. (A) Overall survival from the time of diagnosis of liver metastases to death or to date of last follow-up. (B) Overall survival from the time of diagnosis of the primary UM to death or to date of last follow-up. (C) Disease-free survival from the time of diagnosis of the primary UM to death or to the development of liver metastases. (II) The effects of prognostic factors on survival analysed by the Log Rank test with Kaplan–Meier plots. (A) Overall survival from the time of diagnosis of the primary UM to death or to date of last follow-up: the effects of Cassoux high-risk status (M3/8g). (B) Overall survival from the time of diagnosis of the primary UM to death or to date of last follow-up: the effects of tumour diameter (LTD). (C) Disease-free survival from the time of diagnosis of the primary UM to death or to the development of liver metastases: the effects of Cassoux high-risk status.

replacement pattern, the primary UM had been excluded from the original study [33].

Relationship between HGP and genetic alterations and treatment of metastases

Chi-square analysis failed to demonstrate any significant relationship between the replacement and desmoplastic HGP and loss of chromosome 3 (monosomy 3) and gain in chromosome 8q. In a similar fashion, HGP showed no correlation with various treatments (surgery alone versus surgery plus systemic therapy versus systemic therapy of any kind) administered for metastatic disease or *R* status.

OS after the development of hepatic metastatic disease

Examination of how HGP might potentially influence survival after the development of liver metastases from UM was the primary objective of this study. Univariate analysis with the Log Rank test showed that HGP had a striking effect on OS metastasis ($p = 0.041$) (Figure 5I). In particular, the replacement pattern had a clearly adverse effect on survival versus the

Table 3. Cox proportional hazards analysis for factors predictive of death from time of metastasis

Variables		Univariate		Multivariate	
		HR (95% CI)	*P* value	HR (95% CI)	*P* value
Histopathological growth pattern	Replacement	3.09 (1.02–9.36)	**0.05**	6.51 (1.63–25.92)	**0.008**
Cassoux risk group*	High risk	2.33 (0.85–6.41)	0.1	0.79 (0.22–2.83)	0.720
Largest tumour diameter	>17 mm	2.86 (1.16–7.05)	**0.02**	2.58 (0.86–7.73)	0.091
Treatment	Surgery + systemic	2.17 (0.48–9.81)	0.3	1.04 (0.18–6.07)	0.967
	Systemic	2.61 (0.55–12.33)	0.2	0.80 (0.09–7.21)	0.839
Age	Continuous	1.0 (0.99–1.07)	0.1	1.02 (0.97–1.08)	0.377
Time to metastasis	Continuous	0.82 (0.65–1.03)	0.08	0.74 (0.55–1.00)	**0.05**
R status	*R*1	2.77 (0.57–13.50)	0.21	2.30 (0.42–16.28)	0.307
	*R*2	2.95 (1.14–7.64)	**0.03**	7.94 (1.74–36.18)	**0.007**

*Cassoux risk group: Four genomic groups defined by the status of chromosome 3 and 8: (1) low risk: normal status of chromosomes 3 (disomy 3) and 8 (8nl): D3/8nl, (2) intermediate risk: monosomy 3 and normal status of 8: M3/8nl, (3) intermediate risk: disomy 3 and gain of 8q (8g): D3/8g, and (4) high risk: M3/8g (Tables 1 and 3) [21].
Bold underlined font indicates the *P* values that are statistically significant.

Table 4. Cox proportional hazards analysis for factors predictive of death from date of primary melanoma diagnosis

Variables		Univariate		Multivariate	
		HR (95% CI)	*P* value	HR (95% CI)	*P* value
Histopathological growth pattern	Replacement	2.03 (0.68–6.06)	0.2	4.93 (1.24–19.57)	**0.023**
Cassoux risk group	High risk	3.73 (1.32–10.50)	**0.01**	0.60 (0.17–2.13)	0.43
Largest tumour diameter	>17 mm	4.89 (1.89–12.70)	**0.001**	5.91 (1.96–17.81)	**0.002**
Treatment	Surgery + systemic	3.83 (0.84–17.52)	0.08	1.28 (0.22–7.54)	0.875
	Systemic	3.25 (0.68–15.40)	0.14	5.62 (0.90–35.10)	**0.065**
Age	Continuous	1.04 (1.00–1.08)	**0.04**	1.01 (0.96–1.06)	0.685
Time to metastasis	Continuous	0.58 (0.41–0.82)	**0.002**	0.48 (0.31–0.75)	**0.001**

Bold underlined font indicates the *P* values that are statistically significant.

protective effect of the desmoplastic pattern. The only other variables having significant predictive value for OS on univariate analysis were primary tumour diameter (LTD) ($p = 0.02$) and R (*R*0 complete resection) status ($p = 0.047$). None of the other variables including age, gender, laterality, monosomy 3, 8q gain, the high-risk genomic variable M3/8q gain, melanoma cell type, size of metastasis, and the various treatments for metastatic disease had any significant effect on survival.

On multivariate analysis with the Cox proportional hazards model, HGP continued to show a significant effect with a HR of 6.51 (1.63–25.92) with $p = 0.008$ (Table 3). Conversely, LTD and *R*2 status had HRs of 2.58 (0.86–7.73) ($p = 0.091$) and 7.94 (1.74–36.18) ($p = 0.0071$), respectively, on multivariate analysis. None of the other prognostic factors were significant.

OS analysed from the date of diagnosis of the primary UM

When OS primary is analysed from the date of diagnosis of the primary UM using the Log Rank test, HGP is not statistically significant (Figure 5I). On univariate analysis, other conventional prognostic factors such as patient age, the high risk genomic variable M3/8q gain (Figure 5II), LTD (Figure 5II), and time to metastasis had important predictive value. Monosomy 3 showed borderline significance ($p = 0.052$). No other variables were significant. However, on multivariate analysis, the following were significant: HGP HR 4.93 (1.24–19.57) ($p = 0.023$), tumour diameter 5.91 (1.96–17.81) ($p = 0.002$), and time to diagnosis, but not Cassoux high risk (Table 4).

DFS (metastasis-free) analysis

On univariate analysis, the following prognostic factors were significant: age, monosomy 3, 8q gain, M3/8q gain ($p = 0.008$), and LTD ($p = 0.03$). Examination of HGP in this context of DFS, as expected, appears to have no meaning (Figure 5). On multivariate analysis, none of the variables remained significant (Table 5).

Discussion

In this study, we propose the use of the terms 'replacement and desmoplastic HGP' to describe growth patterns of liver metastases of UM, analogous to those in liver metastases from colorectal (CRC) and breast

Table 5. Cox proportional hazards analysis for factors predictive of metastasis (disease-free survival)

Variables		Univariate		Multivariate	
		HR (95% CI)	*P* value	HR (95% CI)	*P* value
Cassoux risk group	High risk	2.8 (1.32–5.96)	**0.008**	1.87 (0.81–4.31)	0.1
Largest tumour diameter	>17 mm	2.16 (1.09–4.29)	**0.03**	1.57 (0.69–3.55)	0.3
Age	Continuous	1.03 (1.00–1.06)	**0.03**	1.01 (0.98–1.05)	0.5

Bold underlined font indicates the *P* values that are statistically significant.

cancers. Our results are based on international consensus guidelines for the recognition of HGP [21]. It is of interest that independent blinded review of this study set by two pathologists without any knowledge of patient outcome resulted in strikingly good concordance. We believe that this result can be attributed to the recent validation of reliable and reproducible criteria for HGP [21].

For these 41 liver metastases, 30 (73%) were classified as a predominant replacement pattern, while 11 (27%) as a predominant desmoplastic HGP. Our results appear very similar morphologically to those associated with colorectal and breast carcinomas. Further, the observation of comparable morphological findings across multiple tumour types and those with different developmental origins provides additional important support for the biological underpinnings and the generalisability of these HGP in cancer metastases.

Another noteworthy observation from our study that parallels that in other tumour types is that of the prognostic importance of the replacement and desmoplastic growth patterns. In a similar fashion to colorectal and breast carcinoma [21,22], the replacement pattern significantly predicted diminished survival while the desmoplastic pattern correlated with increased survival. These findings potentially provide for the first time an important tissue biomarker for prognosis after the development of liver metastasis. In our study, once metastases have developed, OS diminished significantly ($p = 0.041$) in patients with the replacement pattern. This effect continued to be in significant on multivariate analysis (HR = 7.12, $p = 0.007$). No other factor including 'high-risk' genomic status, i.e. monosomy 3 and 8q gain, had such predictive value. In contrast, as would be expected, HGP had no predictive value for metastasis-free survival or early OS in patients from the time of diagnosis of primary UM in this study population. However, the conventional prognostic factors [patient age (increasing), high-risk genetic status, and primary tumour diameter (LTD)] were significant on univariate analysis after diagnosis of the primary UM but lost this effect on multivariate analysis with the exception of a small effect of LTD ($p = 0.01$). With respect to metastasis-free survival, the genetic variables (monosomy 3, 8q gain, and M3/8q gain) and LTD had important predictive value in the univariate model but were not significant on multivariate analysis. It is of interest that the only patient in this study with normal genetic status (disomy 3, 8q normal), had a metastasis-free interval of 24 years. Following the development and surgical resection of a liver metastasis, this patient has continued to be 'disease-free' at 28 months with a desmoplastic HGP. It is possible that this combination of prognostic factors might prove useful in the management of patients.

The prognostic value of HGPs holds promise for the selection of patients for metastasectomy. At present, only *R*0, i.e. resection for cure, surgical therapy in highly selected patients permits prolonged survival (overall median survival of 27 months with DFS of 10 months) [39]. In contrast, patients with nonresectable liver metastases undergoing the best possible resection of these metastases have a median survival of only 15 months. However, there is no correlation between *R* status and any type of HGP, and HGP continues to be important on multivariate analysis even after adjustment for *R* status (Table 3). Thus it of interest that HGPs may provide important prognostic information about all patient groups with liver metastases, irrespective of *R*0 status. An ultimate goal is the correlation of radiological images with HGPs which could provide a noninvasive means of selecting patients for metastasectomy or medical therapy.

The frequency of the replacement and desmoplastic patterns in our study differs from the frequencies observed in colorectal and breast carcinomas. As compared to our results, colorectal carcinoma appears to show a greater frequency of desmoplastic HGP, whereas breast carcinoma shows an almost exclusive replacement pattern [21,22]. In any event, the predominance of the replacement pattern observed in liver metastases from UM may be directly related to or predictive of the overall adverse prognosis associated with this neoplasm. In addition, as in CRC [22], the appearance of new liver metastases and/or the more rapid death of patients with UM may potentially be linked to the transformation of established metastases with the desmoplastic pattern to a mixed pattern with replacement. Future studies are

needed to establish if this potentially adverse evolution in HGP occurs in UM.

Concerning this adverse evolution linked to the replacement pattern, it is important to emphasise that, in the replacement pattern (angiotropism/vascular co-option), tumour cells occupy 'vascular niches', such as the space of Disse [4]. Accumulating evidence suggests that this perivascular space is a preferential niche for cancer stem cells (or cells with stem cell properties), resistance to therapy, protection or escape from the immune response, i.e. an immunologically privileged site, and the progression and dissemination of cancer [4,22,40–44].

With particular reference to the replacement HGP in this study, immunohistochemistry and EM have confirmed that the melanoma cells located in the vicinity of sinusoidal vessels are localised to the abluminal vascular surfaces of sinusoidal vessels and in the space of Disse, rather than being intraluminal [45,46]. These findings provide additional support for the concept that vascular co-option and angiotropism/EVMM is inherently an 'extravascular' (abluminal) phenomenon and independent of intravasation. It is of interest that, in the previous autopsy studies of Grossniklaus *et al* [4], their 'infiltrative' cases thought to correspond to the replacement HGP in fact showed intrasinusoidal involvement by melanoma cells, a finding never seen in our current work.

Finally, concerning the migratory pathway of angiotropic tumour cells, several *in vitro* and *in vivo* observations have demonstrated that angiotropic melanoma cells in cutaneous melanoma are able to migrate some distance from the primary tumour [7,25,34]. Since the 19th century, the migration of tumour cells along vessels and other tracks without intravasation has been described [10–13,47]. However, additional studies are needed to confirm distant metastasis by this migratory route.

The lack of correlation between monosomy 3 and 8q gain and liver HGP in UM and the lack of prognostic significance of these genetic factors in the context of UM liver metastases prompts some discussion. First of all, these observations suggest that different mechanisms may be operative in the metastatic process of UM, at least for liver metastases. It is of interest that in a previous study there was no correlation between angiotropism in primary UM and monosomy 3 [33]. 8q gain was not examined in that study. The best explanation may be that the molecular basis of vascular co-option/EVMM simply has not yet been established and that more investigation is needed, including larger patient cohorts.

As mentioned earlier, recent autopsy studies have referred to metastatic deposits as 'infiltrative' and 'nodular' [5,15]. The question arises as to whether the latter descriptions bear any resemblance or relationship to the replacement, desmoplastic, and pushing HGPs observed in the current study. This 'infiltrative' pattern [4] seems to have features of both the replacement and desmoplastic HGPs in this study as melanoma cells 'infiltrate' hepatocytes (infiltrative, stages I and II [6]) as in our replacement HGP and they may form expansive tumour aggregates surrounded by fibrous septae (infiltrative, stage III [4]), as our desmoplastic HGP. Conversely, the 'nodular' pattern [4] exhibits both angiotropism of melanoma cells to portal venules (and the space of Disse), a feature associated with the replacement HGP in our study, and cohesive tumoural aggregates that compress and obliterate the liver parenchyma, a defining characteristic of the pushing HGP. How can one account for these differences? First of all, there are striking differences between the two studies. A fundamental difference is the nature of the material selected for study – autopsy versus material derived from the surgical resection of liver metastases identified by radiological imaging (MRI) in living patients with UM. Autopsy material is clearly marked by an advanced and terminal stage of disease versus an earlier stage of disease assessed in our cohort of living patients. Furthermore, autopsy material may be suboptimal. One major difference in our study was the apparent absence of intraluminal sinusoidal involvement by metastatic UM. Importantly, intravascular/intrasinusoidal tumour cells are seen more frequently in autopsy material than in living patient samples [21,48]. In addition, the case material studied by Grossniklaus *et al* may to some degree correspond to what has been termed 'diffuse intrasinusoidal metastatic disease' as seen in the context of rare aggressive cancers or in autopsy material [21,49,50]. Furthermore, the foci of liver involvement by UM in Grossniklaus' studies ranged from <0.05 to 0.5 mm in diameter or larger; while our metastases ranged from approximately 1–17 mm (mean and median about 6 mm) in diameter. Sample size differences, i.e. $n = 15$ versus $n = 41$, between the two studies may also be a factor to consider in making comparisons difficult. Finally, all of the latter considerations and the use of the international consensus guidelines for classifying metastases in our study and in particular the primacy of the metastasis-liver interface would appear to indicate that these two studies are fundamentally different.

In conclusion, we report for the first time the frequency of the replacement and desmoplastic HGPs in liver UM metastases resected from living patients, and their potential important prognostic value for UM

patients, as in other solid cancers. With additional study, these results may potentially be utilised to develop objective radiological correlates and therapeutic targets for managing patients with UM metastases.

Acknowledgements

This work was supported by the French National Research Agency through the 'Investments for the Future' program (France-BioImaging, ANR-10-INSB-04). We acknowledge the PICT-IBiSA, member of the France-BioImaging national research infrastructure, supported by the CelTisPhyBio Labex (N° ANR-10-LBX-0038) part of the IDEX PSL (N°ANR-10-IDEX-0001-02 PSL).

Author contributions statement

RB, PV, and CL designed the study, developed the methodology, performed experiments, collected data, and analysed data. RB and CL wrote the manuscript. SD developed the methodology, collected and analysed data. P-JVD, PV, and SD performed statistical analyses and analysed data. IH and GR performed and interpreted electron microscopy. AN performed immunohistochemistry and scanned glass slides and managed glass microslides. GP directed and analysed array comparative hybridisation. PM and SPN collected data. SPN analysed data. All the authors reviewed and approved the manuscript.

References

1. Amaro A, Gangemi R, Piaggio F, *et al*. The biology of uveal melanoma. *Cancer Metastasis Rev* 2017; **36:** 109–140.
2. Farquhar N, Thornton S, Coupland SE *et al*. Patterns of BAP1 protein expression provide insights into prognostic significance and the biology of uveal melanoma. *J Pathol Clin Res* 2017; **4:** 26–38.
3. Diener-West M, Reynolds SM, Agugliaro DJ, *et al*. Development of metastatic disease after enrollment in the COMS trials for treatment of choroidal melanoma: Collaborative Ocular Melanoma Study Group Report No. 26. *Arch Ophthalmol* 2005; **123**:1639–43.
4. Grossniklaus HE, Zhang Q, You S, *et al*. Metastatic ocular melanoma to the liver exhibits infiltrative and nodular growth patterns. *Hum Pathol* 2016; **57**: 165–175.
5. Borthwick NJ, Thombs J, Polak M, *et al*. The biology of micrometastases from uveal melanoma. *J Clin Pathol* 2011; **64**:666–671
6. Blanco PL, Lim LA, Miyamoto C, *et al*. Uveal melanoma dormancy: An acceptable clinical endpoint? *Melanoma Res* 2012; **22**: 334–40.
7. Lugassy C, Zadran S, Bentolila LA, *et al*. Angiotropism, pericytic mimicry and extravascular migratory metastasis in melanoma: An alternative to intravascular cancer dissemination. *Cancer Microenviron* 2014; **7**: 139–52.
8. Bald T, Quast T, Landsberg J *et al*. Ultraviolet radiation-induced inflammation promotes angiotropism and metastasis in melanoma. *Nature* 2014; **6**; 507: 109–13.
9. Landsberg J, Tüting T, Barnhill RL, *et al*. The role of neutrophilic inflammation, angiotropism, and pericytic mimicry in melanoma progression and metastasis. *J Invest Dermatol* 2016; **136**: 372–7.
10. Récamier JCA (1829) In: *Recherches sur le traitement du cancer*. Gabon, Paris
11. Friedl P, Alexander S. Cancer invasion and the microenvironment: Plasticity and reciprocity. *Cell* 2011; **147**: 992–1009.
12. Gritsenko P, Leenders W, Friedl P. Recapitulating in vivo-like plasticity of glioma cell invasion along blood vessels and in astrocyte-rich stroma. *Histochem Cell Biol* 2017; **148**: 395–406.
13. Levy MJ, Gleeson FC, Zhang L. Endoscopic ultrasound fine needle aspiration detection of extravascular migratory metastasis from a remotely located pancreatic cancer. *Clin Gastroenterol Hepatol* 2009; **7**: 246–248.
14. Holmgren L, O'Reilly MS, Folkman J. Dormancy of micrometastases: Balanced proliferation and apoptosis in the presence of angiogenesis suppression. *Nat Med* 1995; **1**: 149–53.
15. Grossniklaus HE. Progression of ocular melanoma metastasis to the liver: The 2012 Zimmerman lecture. *JAMA Ophthalmol* 2013; **131**: 462–9.
16. Liao A, Mittal P, Lawson DH, *et al*. Radiologic and histopathologic correlation of different growth patterns of metastatic uveal melanoma to the liver. *Ophthalmology* 2018; **125**: 597–605.
17. Van den Eynden GG, Majeed AW, Illemann M *et al*. The multifaceted role of the microenvironment in liver metastasis: Biology and clinical implications. *Cancer Res* 2013; **73**: 2031–43.
18. Vermeulen PB, Colpaert C, Salgado R, *et al*. Liver metastases from colorectal adenocarcinomas grow in three patterns with different angiogenesis and desmoplasia. *J Pathol* 2001; **195**: 336–42.
19. Van den Eynden GG, Bird NC, Majeed AW *et al*. The histological growth pattern of colorectal cancer liver metastases has prognostic value. *Clin Exp Metastasis* 2012; **29**: 541–9.
20. Nielsen K, Rolff HC, Eefsen RL, *et al*. The morphological growth patterns of colorectal liver metastases are prognostic for overall survival. *Mod Pathol* 2014; **27**: 1641–8.
21. van Dam PJ, van der Stok EP, Teuwen LA, *et al*. International consensus guidelines for scoring the histopathological growth patterns of liver metastasis. *Br J Cancer* 2017; **117**: 1427–1441.
22. Frentzas S, Simoneau E, Bridgeman VL, *et al*. Vessel co-option mediates resistance to anti-angiogenic therapy in liver metastases. *Nat Med* 2016; **22**:1294–1302.
23. Barnhill R, Dy K, Lugassy C. Angiotropism in cutaneous melanoma: A prognostic factor strongly predicting risk for metastasis. *J Invest Dermatol* 2002; **119**:705–6.
24. Barnhill RL, Lugassy C. Angiotropic malignant melanoma and extravascular migratory metastasis: Description of 36 cases with emphasis on a new mechanism of tumour spread. *Pathology* 2004; **36**: 485–90.
25. Bentolila LA, Prakash R, Mihic-Probst D, *et al*. Imaging of angiotropism/vascular co-option in a murine model of brain melanoma:

Implications for melanoma progression along extravascular pathways. *Sci Rep* 2016; **6**: 23834.
26. Starr HJ, Zimmerman LE. Extrascleral extension and orbital recurrence of malignant melanomas of the choroid and ciliary body. *Int Ophtalmol Clin* 1962; **2**: 369–384.
27. Shammas HF, Blodi FC. Orbital extension of choroidal and ciliary body melanomas. *Arch Ophthalmol* 1977; **95**: 2002–2005.
28. Affeldt JC, Minckler DS, Azen SP, *et al*. Prognosis in uveal melanoma with extrascleral extension. *Arch Ophthalmol* 1980; **98**: 1975–1979.
29. Seddon JM, Albert DM, Lavin PT, *et al*. A prognostic factor study of disease-free interval and survival following enucleation for uveal melanoma. *Arch Ophthalmol* 1983; **101**: 1894–9.
30. Zografos L. *Tumeurs intraoculaires*. Paris: Masson; 2002: 236–51.
31. Coupland SE, Campbell I, Damato B. Routes of extraocular extension of uveal melanoma: Risk factors and influence on survival probability. *Ophthalmology* 2008; **115**: 1778–1785.
32. Kizhatil K, Ryan M, Marchant JK, *et al*. Schlemm's canal is a unique vessel with a combination of blood vascular and lymphatic phenotypes that forms by a novel developmental process. *PLoS Biol* 2014; **12**: e1001912.
33. Barnhill RL, Ye M, Batistella A, *et al*. The biological and prognostic significance of angiotropism in uveal melanoma. *Lab Invest* 2017; **97**: 746–59.
34. Van Es SL, Colman M, Thompson JF, *et al*. Angiotropism is an independent predictor of local recurrence and in-transit metastasis in primary cutaneous melanoma. *Am J Surg Pathol* 2008; **32**: 1396–403.
35. Wilmott J, Haydu L, Bagot M, *et al*. Angiotropism is an independent predictor of microscopic satellites in primary cutaneous melanoma. *Histopathology* 2012; **61**: 889–98.
36. Cassoux N, Rodrigues MJ, Plancher C, *et al*. Genome-wide profiling is a clinically relevant and affordable prognostic test in posterior uveal melanoma. *Br J Ophthalmol* 2014; **98**: 769–774.
37. McLean IW, Burnier MN, Zimmerman LE, *et al*. Atlas of tumor pathology: Tumors of the eye and ocular adnexa. Armed Forces Institute of Pathology: Washington DC, USA, 1994; 179–191.
38. Pourhoseingholi MA, Baghestani AR, Vahedi M. How to control confounding effects by statistical analysis. *Gastroenterol Hepatol Bed Bench* 2012; **5**: 79–83.
39. Mariani P, Piperno-Neumann S, Servois V, *et al*. Surgical management of liver metastases from uveal melanoma: 16 years' experience at the Institut Curie. *Eur J Surg Oncol* 2009; **35**: 1192–7.
40. Borovski T, De Sousa E Melo F, *et al*. Cancer stem cell niche: The place to be. *Cancer Res* 2011; **71**: 634–9.
41. Lu J, Ye X, Fan F, *et al*. Endothelial cells promote the colorectal cancer stem cell phenotype through a soluble form of Jagged-1. *Cancer Cell* 2013; **23**: 171–85.
42. Lugassy C, Péault B, Wadehra M, *et al*. Could pericytic mimicry represent another type of melanoma cell plasticity with embryonic properties? *Pigment Cell Melanoma Res* 2013; **26**: 746–54.
43. Lugassy C, Scolyer R, Long G, *et al*. PDGFBR expression in anti-BRAF resistant melanoma: Are angiotropic melanoma cells a source of BRAF resistance and disease progression? *J Cutan Pathol* 2014: **41**: 159–160.
44. Winkler F. Hostile takeover: How tumours hijack pre-existing vascular environments to thrive. *J Pathol* 2017; **242**: 267–272.
45. Lugassy C, Eyden BP, Christensen L, *et al*. Angio-tumoral complex in human malignant melanoma characterised by free laminin: Ultrastructural and immuno-histochemical observations. *J Submicrosc Cytol Pathol* 1997; **29**: 19–28
46. Lugassy C, Dickersin GR, Christensen L, *et al*. Ultrastructural and immunohistochemical studies of the periendothelial matrix in human melanoma: Evidence for an amorphous matrix containing laminin. *J Cutan Pathol* 1999; **26**: 78–83.
47. Griveau A, Seano G, Shelton SJ, *et al*. A glial signature and Wnt7 signaling regulate glioma-vascular interactions and tumor microenvironment. *Cancer Cell* 2018; **33**: 874–889.e7
48. Sykes AM. Intravascular tumor emboli. In: *Pearls and Pitfalls in Thoracic Imaging: Variants and Other Difficult Diagnoses*, Hartman T (ed). Cambridge University Press: Cambridge, 2011; 148–149.
49. Allison KH, Fligner CL, Parks WT. Radiographically occult, diffuse intrasinusoidal hepatic metastases from primary breast carcinomas: A clinicopathologic study of 3 autopsy cases. *Arch Pathol Lab Med* 2004; **128**: 1418–23.
50. Simone C, Murphy M, Shifrin R, *et al*. Rapid liver enlargement and hepatic failure secondary to radiographic occult tumor invasion: Two case reports and review of the literature. *J Med Case Rep* 2012; **6**: 402.